Surface morphology of He-implanted single-crystalline silicon[*]

LI Bing-Sheng(李炳生)[1,2;1)]　　ZHANG Chong-Hong(张崇宏)[1]

ZHOU Li-Hong(周丽宏)[1,2]　　YANG Yi-Tao(杨义涛)[1,2]

1 (Institute of Modern Physics, Chinese Academy of Sciences, Lanzhou 730000, China)

2 (Graduate School of Chinese Academy of Sciences, Beijing 100049, China)

Abstract　Single-crystalline Si (100) samples were implanted with 30 keV He^{2+} ions to doses ranging from 2.0×10^{16} to 2.0×10^{17} ions /cm^2 and subsequently thermally annealed at 800 ℃ for 30min. The morphological change of the samples with the increase of implantation dose was investigated using atomic force microscopy (AFM). It was found that oblate-shaped blisters with an average height around 4.0nm were found on the 2.0×10^{16} ions /cm^2 implanted sample surface; spherical-shaped blisters with an average height around 10.0nm were found on the 5.0×10^{16} ions /cm^2 implanted sample surface; strip-shaped and conical cracks were observed on the sample He-implanted to a dose of 1.0×10^{17} ions /cm^2. Exfoliations occurred on the sample surface to a dose of 2.0×10^{17} ions /cm^2. Mechanisms underlying the surface change were discussed.

Key words　crystalline silicon, He ion implantation, He bubble, Cavities, blisters, morphology

PACS　61.72.-y, 61.80.-x, 61.82.Fk

1　Introduction

Irradiation of silicon with light ions has been studied for many years. In particular, helium is known to agglomerate into bubbles after being implanted in silicon. When helium ions were injected into silicon above a critical dose, helium bubbles were found in the near surface region and can evolve into nanometric voids via helium out-diffusion during subsequent thermal annealing[1]. Currently, it is great interesting to apply the nanometric voids in the silicon device technology, because of that nanometric voids can be used as powerful getting centers of transition metals atoms[2—4]. The cavity internal surface can also interact strongly with point defects such as interstitials and vacancies, so that it can play significant role on dopant diffusivity and suppression of secondary defects[5—6]. In addition, cavities introduce deep lev-els in the silicon band gap that can be used to control lifetime of carriers in silicon power devices[7—8]. The increasing interest on possible applications in silicon device technology has also stimulated investigations on the basic mechanisms underlying cavity formation and evolution[9]. A detail understanding is clearly necessary to control the cavities effects and their interaction with neighboring structures.

Cavities can be formed in silicon by high-dose helium implantation and subsequent annealing. It was observed by transmission electron microscopy (TEM) that neighborhood of the cavities have great strains which lead to the formation of dislocation loop, stacking defects etc[10]. In addition, the strains can accumulate at the region above the amorphous layer and even can result in blisters at the surface[11], which will give negative effects on development of the Super Large-Scale Integration (SLSI).

It has been widely accepted that ion beam implantation can result in a change of the surface morphology, such as roughening or smoothing of the surface[12—14]. Important factors like ion beam energy, ion mass, incident angle, ion flux, dose, substrate temperature and annealing temperature will determine the effect on the surface morphology. In the present work, the ion dose was varied while other parameters were kept constant was studied, in order to understand the surface morphology evolution of silicon with He-ion dose.

2   Experimental

P-type Czochralski (100) silicon wafers ($\geq 1\Omega$cm)

were implanted with He^{2+} ions at 30 keV with different doses ranging from 2.0×10^{16} to 2.0×10^{17} ions/cm^2 at 300 ℃. The dose rate was 2×10^{13} ions/cm^2·s. Annealing at 800 ℃ was performed in vacuum for 30min in a quartz tube within a tubular furnace. Atomic Force Microscopy (Shimadzu, SPM-9500) was used to study the surface morphology of the samples.

3   Results

Figure 1 shows the AFM images of the sample's surface. The sample conditions are given in the Fig. 1. It is clearly seen that the surface morphology changed significantly with the increase of the He-implantation dose.
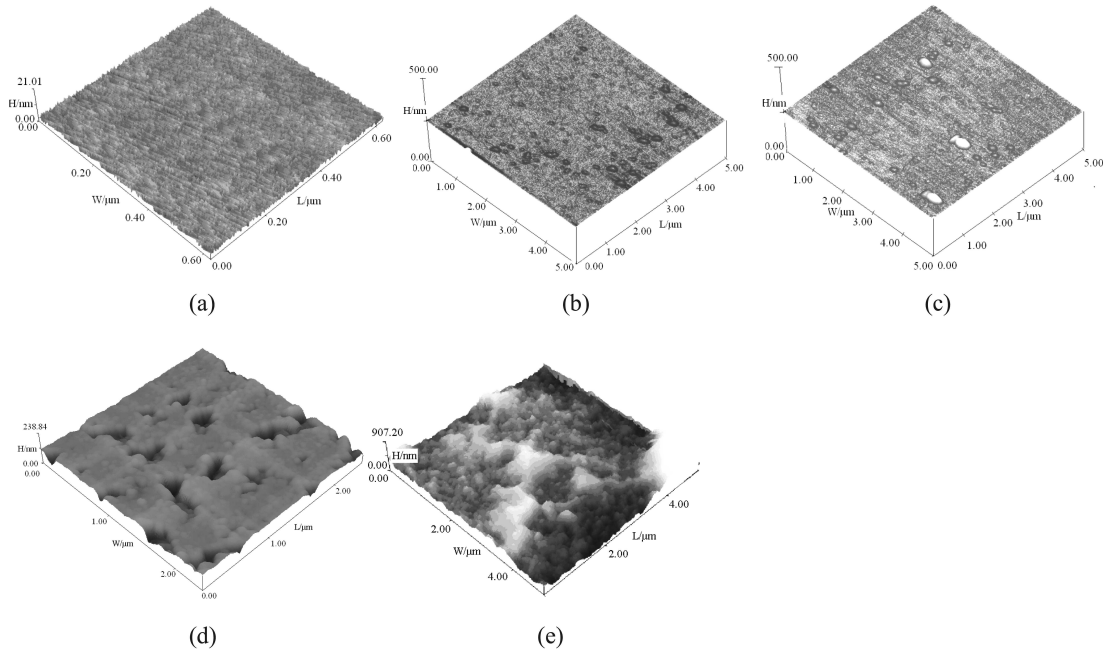

Fig. 1.   Typical AFM images (a)—(e) of Si (100) surfaces varying with helium implantation doses. (a) Pristine Si, (b)—(e) are respectively 2.0×10^{16}, 5.0×10^{16}, 1.0×10^{17}, 2.0×10^{17}cm^{-2} He-implanted samples followed by thermal annealing at 800 ℃ for 30min in vacuum.

In detail, the surface of the pristine Si is quite smooth (Fig. 1(a)), with increasing He- implantation dose, the surface roughness increased gradually; non-continuous distribution of oblate-shaped blisters have an average height around 4.0 nm (Fig. 1(b)); spherical-shaped blisters have an average height around 10 nm and appeared with a few blisters with height around 30 nm (Fig. 1(c)); strip-shaped and conical cracks have an average depth around 70 nm and appear with a high density of the spherical-like blisters (Fig. 1(d)); non-continuous distribution of ex-

foliations have a maximum depth approaching 700 nm (Fig. 1(e)).

4   Discussion

He ions implanted into Si produce vacancy defects. At the early stages of the implantation process the helium atoms are sufficiently mobile even at room temperature to reach the vacancies or vacancies clusters produced by He ions implantation to form helium-vacancy ($He_m V_n$) complexes[15]. It has

been shown that the accumulation of helium in silicon up to a dose of 3.5×10^{20} He/cm^3[16] would result in the formation of helium bubbles in silicon. According to SRIM-1996[17] calculation, 30 keV He ions injected into silicon to doses ranging from 2.0×10^{16} to 2.0×10^{17} ions /cm^2, with an estimated R_p=339 nm and ΔR_p=100 nm, could lead to maximal local He concentrations ranging from 8.0×10^{20} to 8.0×10^{21} He/cm^3, which are well above the minimum concentration required for the bubble formation after annealing.

The coalescence and growth of gas bubbles may occur in the presence of many neighboring He atoms and Si lattices vacancies. The equilibrium pressure p, balancing the surface tension of a spherical cavity is given by[18]:

$$p = \frac{2\gamma}{r} \ , \tag{1}$$

where γ is the surface free energy of the bubble. It has a value of 1.3 J/m^2 in silicon (an average over the (111), (100), (311) and (110) facets). If the radius of a bubble is 2 nm, an equilibrium pressure is 6.5×10^8 Pa. This is a quite-high pressure which will cause plastic deformation near the sample surface. For example, it may show the cracks on the sample surface.

Freund[19] reported a critical pressure for crack growth as follows:

$$p = \mu \left(\frac{\pi \gamma}{(1-\nu)a\mu} \right)^{1/2} \ , \tag{2}$$

where a single crack in Si with shear modulus μ and Poisson ratio ν. The crack edge is taken to be circular of radius a. It can be seen that from Eq. (2) that the pressure required in the crack cavity to sustain crack growth decreases as the crack size increases.

During the formation of the blisters[20], two stages are involved. At the first stage, the diffusion of helium and vacancies towards bubbles occurred parallel to the surface, resulting in over-pressure helium bubbles. At the second stage, de-sorption of helium from smaller bubbles occurred, resulting in both the dissolution of small cavities and growth of the larger ones. When the size of a cavity reaches micrometer, the cavity causes plastic deformation near the sample surface to form round and domed blisters as shown in Fig. 1(b) and Fig. 1(c).

Because the sample implantation dose of Fig. 1(c) is larger than that of Fig. 1(b), the sample is supposed to have higher density and larger shape cavities in the Fig. 1(c). Meanwhile, more He atoms may enter the bubbles and cause higher pressure. Therefore, the sample in Fig. 1(c) contains larger blisters in higher number density on the surface than that of Fig. 1(b). When the implantation dose is up to 1.0×10^{17} ions/cm^2, the over-pressure bubbles formed in the samples can lead to the burst of the surface blisters[21], thus may make cracks on the surface (Fig. 1(d)).

When implantation dose of helium ions reaches a higher fluence of 2.0×10^{17} ions /cm^2, gas bubbles in the largest size and the highest density will be formed, which could have caused a big average radius of crack. According to Eq. (2), in such a condition critical pressure sustains growth of crack can be easily met, and may lead to lateral cracks in the sample. When the lateral cracks were large enough, they may produce a large-area exfoliation in the sample as shown in Fig. 1(e). The whole process of the surface morphology evolution can be illustrated as in Fig. 2.
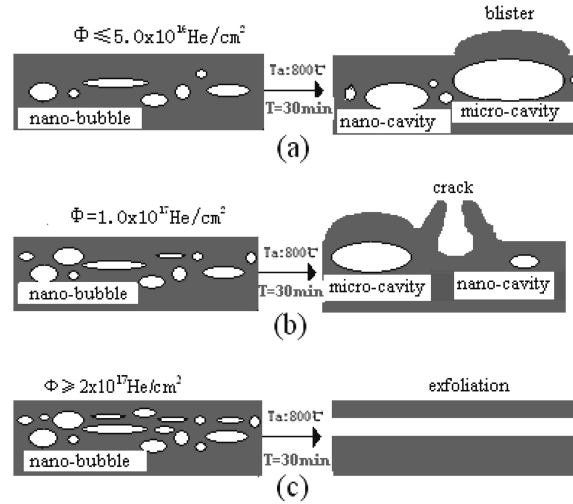

Fig. 2. Sketch diagram showing the surface morphology evolution with different doses helium ions implanted silicon followed by thermal annealing at 800 ℃ for 30 min.

5 Conclusion

In this work we used AFM to investigate the morphological modification of mono-crystalline Si(100) surface by helium implantation followed by thermal annealing at 800 ℃. The nano-roughness of the implantation surfaces are evaluated and compared before and after implantation. At a dose of 2.0×10^{16} ions/cm^2, small oblate blister-like structures appear on the sample's surface. The in-

crease of implantation dose up to 5.0×10^{16} ions/cm^2 leads to a larger population of spherical blisters. However, the increase of implantation dose up to 1.0×10^{17} ions/cm^2 leads to a lot of cracks surrounded by abundant spherical blisters. Further increase of implantation dose up to 2.0×10^{17} ions/cm^2 leads to the exfoliation of the sample's surface. It is regarded that the formation of over-pressure helium bubbles and micro-cavities can lead to the dramatic change on the sample surface.

References

1 Tonini R, Corni F, Frabboni S et al. J. Appl. Phys., 1998, **84**: 4802
2 Kinomura A, Horino Y, Nakano Y et al. J. Appl. Phys., 2005, **98**: 066102
3 ZHANG Miao, ZENG Xu-Chu, Chu Paul K et al. J. Appl. Phys., 1999, **86**: 4214
4 Wong-Leung J, Williams J S, Kinomura A et al. Phys. Rew. B, 1999, **59**: 7990
5 Raineri V, Campisano S U. Appl. Phys. Lett., 1996, **69**: 1783
6 Raineri V, Campisano S U. Nucl. Instrum. Methods B, 1996, **120**: 56
7 Seager C H, Myers S M, Anderson R A et al. Phys. Rew. B, 1994, **50**: 2458
8 Raineri V, Fallica P G, Percolla G et al. J. Appl. Phys., 1995, **78**: 3727
9 Evans J H. Nucl. Instrum. Methods B, 2002, **196**: 125
10 Avic Ibrahim, Law Mark. E, Kuryliw Erik et al. J. Appl. Phys., 2004, **95**: 2452
11 Fabnroni S, Gazzadi G C, Felisari L et al. Appl. Phys. Lett., 2004, **85**: 1683
12 Muto S, Matsui T, Tanabe T, J. Nucl. Mater, 2001, **290-293**: 131
13 QIAN C, Terreault B, Gujrathi S C. Nucl. Instrum. Methods B, 2001, **175—177**: 711
14 Boldyryeva H, Kishimoto N, Umeda N et al. Nucl. Instrum. Methods B, 2004, **219—220**: 953
15 Oliviero E, Beaufort M F, Barbot J F et al. J. Appl. Phys., 2001, **89**: 5332
16 Raineri V, Coffa S, Szilagyi E et al. Phys. Rev. B, 2000, **61**: 937
17 Ziegler J F, Biersack J P, Littmark U. The stopping and range of Ions in Solids, Vol.1, Pergamon press, New York, 1984
18 Hastings, Estreicher R, Feldman L C et al. Phys. Rev. Lett., 1993, **70**: 1643
19 Freund L B. Appl Phys. Lett., 1997, **70**: 3519
20 Frabboni S, Corni F, Nobili C et al. Phys. Rev. B, 2004, **69**: 165209
21 Moreno D, Eliezer D. Metallurgical and Materials Transactions A, 1997, **28**: 755